Fuel Cells DOI: 10.1002/fuce.201600222

ORIGINAL RESEARCH PAPER

Relation Between Ni Particle Shape Change and Ni Migration in Ni–YSZ Electrodes – a Hypothesis▲

M. B. Mogensen[1]*, A. Hauch[1], X. Sun[1], M. Chen[1], Y. Tao[1], S. D. Ebbesen[1], K. V. Hansen[1], P. V. Hendriksen[1]

[1] Department of Energy Conversion and Storage, Technical University of Denmark (DTU), Frederiksborgvej 399, DK-4000 Roskilde, Denmark

Received November 21, 2016; accepted February 24, 2017; published online May 29, 2017

Abstract

This paper deals with degradation mechanisms of Ni–YSZ electrodes for solid oxide cells, mainly solid oxide electrolysis cells (SOECs), but also to some extent solid oxide fuel cells (SOFCs). Analysis of literature data reveals that several apparently different and even in one case apparently contradicting degradation phenomena are a consequence of interplay between loss of contact between the Ni–YSZ (and Ni–Ni particles) in the active fine-structured composite fuel electrode layer and migration of Ni via weakly oxidized Ni hydroxide species. A hypothesis that unravels the apparent contradiction and explains qualitatively the phenomena is presented, and as a side effect, light has been shed on a degradation phenomenon in solid oxide fuel cells (SOFCs) that has been observed during a decade.

Keywords: Degradation, Electrode, Energy Conversion, Fuel Cell, Ni/YSZ, SOEC, SOFC

1 Introduction

Solid oxide electrolysis cells (SOECs) must be developed to a stage where their lifetime lasts several years under operating conditions with a current density of –1 A cm^{-2} or higher. This is necessary in order to decrease the cost of the installed electrolyzer capacity in terms of Nm^3 hydrogen (or syngas) produced per hour. Therefore, DTU Energy has been carrying out a comprehensive program on SOEC cell development and testing of SOECs at high current densities over long periods during recent years [1–10]. Indeed, several other laboratories have also contributed to the testing of SOEC durability, e.g., European Institute for Energy Research, Forschungszentrum Jülich and Idaho National Laboratory [11–14]. A literature search reveals that more than 40 papers about SOEC long term degradation are available, but it is outside the scope of this paper to review all the relevant literature, and the readers are referred to the reviews [2, 13].

The mentioned papers report and explain a number of failure modes. However, there was one of the observed new degradation phenomena of highly polarized SOEC Ni–YSZ cermet fuel electrodes, which we had some difficulties to explain. We observed repeatedly a significant loss of Ni from the part of the Ni–YSZ cathode layer closest to the electrolyte in spite of the fact that we previously have observed and explained that Ni may migrate towards the electrolyte under circumstances of high temperature (950 °C) and current density (down to –1 A cm^{-2}, 67% H_2O – 33% H_2 feed) [1]. Based on [1] and other literature [15–18] we would expect movements of $Ni(OH)_x$, as illustrated in Figure 1. We denote the migrating Ni species $Ni(OH)_x$, because the precise composition of the migrating compound is still uncertain, but we know for sure that it migrates down steam partial pressure, pH_2O, gradients. In the context of solid oxide cells (SOCs) it means that Ni is expected to migrate outwards in SOFCs and inwards in SOECs as illustrated in Figure 1. It is worth noting

▲ *Paper presented at the 12th EUROPEAN SOFC & SOE FORUM (EFCF2016), July 5–8, 2016 held in Lucerne, Switzerland. Organized by the European Fuel Cells Forum www.efcf.com*

[*] *Corresponding author, momo@dtu.dk*

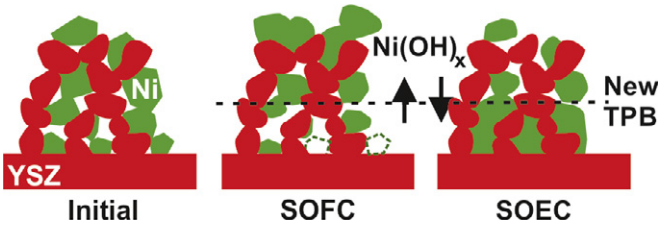

Fig. 1 Illustration of the expected Ni migration directions and consequent changes of the microstructure in case of stable electrical contact between Ni and YSZ with simultaneous open paths for electrons, oxide ions and H_2O and H_2 molecules. In both cases the electrode degrades as the TPB moves outwards from the electrolyte and the small Ni particles are removed or overgrown, respectively, with the consequence that both R_s and R_p increase.

that in both cases this gives rise to degradation mechanisms which involve an increase in the series resistance of the cell, because in both cases the active three phase boundary length (TPB) moves outwards as shown in Figure 1.

In case of SOECs, in which a loss of Ni in the innermost part of the electrode was observed, the general trend was a polarization resistance increase during the first few hundred hours and, more detrimental on the long-term scale, a significant and almost linear increase in ohmic (series) resistance. The consequence was serious performance degradation.

On this basis our question was: how can the Ni migrate the opposite way with the same current density just 100–150 °C lower than the test reported by us earlier in [1]? Some brief explanation of the phenomenon has recently been published by some of us (YT, SDE, MBM) as part of a paper reporting on durability measurements [19]. In the present paper we describe in more details hypotheses and some evidence for the mechanisms of first the loss of contact between Ni and YSZ particles and Ni–Ni particles in the electrochemically active cermet electrode layer. The loss of contact between the Ni–YSZ must take place before the Ni migration away from the electrolyte can start. Actually, our analysis tells that the loss of contact is the main event for the degradation of the Ni–YSZ electrode during the first few hundred hours, and this degradation due to loss of Ni–YSZ particle contact is also observed in SOFC mode [17, 20].

2 Observations

Detailed descriptions of experimental procedures, such as cell manufacturing, cell test set-up, reduction profiles, test conditions, electrochemical characterization *via* impedance spectroscopy and characterization *via* scanning electron microscopy (SEM) can be found, e.g., in the recent publication by Hauch et al. [10] and references cited herein. Details on specific cells and test conditions for the examples shown in here can be found in the references cited along with the figures and descriptions given in this work. Furthermore, a description of the low-voltage scanning electron microscopy (LV-SEM) imaging technique applied for the SEM images in Figures 3, 4 and 6 can be found in the work by Thydén et al. [21].

2.1 Electrolysis Test Results

Figure 2 shows SEM micrographs which illustrate important aspects of the changes observed in an early stage of the migration of Ni against the steam gradient in a Ni–YSZ cermet during SOEC tests at high current density. Figure 2A is a micrograph of a pristine SOEC cathode structure produced *via* multilayer tape casting of all layers of the half-cell [22] and Figure 2B is a micrograph from a sister cell to the cell in Figure 2A but tested for 1,000 h at –1.25 A cm^{-2}, 90% H_2O in inlet, 56% conversion and 800 °C [10].

The development of cell voltage, the series resistance, R_s, and the electrode polarization resistance, R_p, during the long-term test conducted for the cell depicted in Figure 2B is given in the work by Hauch et al. as Figure 7, "Cell D" [10]. From this work it was observed that R_s was more or less constant during the first 300 h but over the entire test period of 1,000 h R_s increased by approximately 115 mΩ cm^2 from 105 mΩ cm^2 to 225 mΩ cm^2. In this long-term tested cathode the Ni particles seem to have lost contact to each other as well as to the YSZ particles in the cathode cermet next to the electrolyte. Please note that the Ni particles that have lost contact seem more rounded than in the initial structure in Figure 2A. It is also observed that the Ni particles in the inactive support have become rounded to some extent, but contact is clearly not lost.

Figure 3 shows representative LV-SEM micrographs of Ni–YSZ electrodes and Ni–YSZ cell support layers. The four features seen are: (i) the white particles, which are electrically interconnected Ni particles with contact to ground in the SEM, (ii) the light gray particles are Ni particles that have lost contact to each other, (iii) the dark gray particles are YSZ, and the black features are porosity.

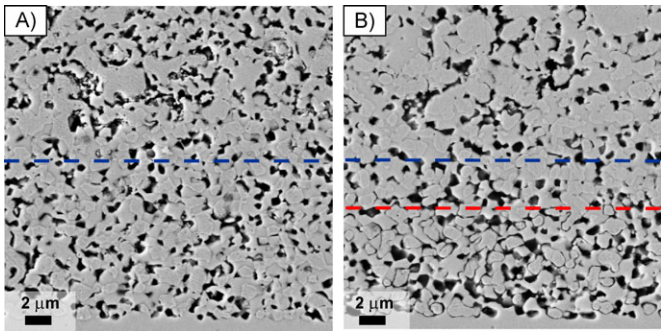

Fig. 2 SEM micrographs of Ni–YSZ electrodes. A) Micrograph of the pristine Ni–YSZ electrode of a reference cell (not long term tested, only reduced and initially characterized) [22]. B) Micrograph of a sister cell to Figure 2A but tested for 1,000 h at –1.25 A cm^{-2}, 90% H_2O in inlet, 56% conversion and 800 °C [10]. The Figure is reproduced by permission of Elsevier. The blue dashed line indicates the border between the active fuel electrode (Ni/8YSZ) and the support layer (Ni/3YSZ) while the red dashed line in B) guides the eye to the part of the fuel electrode where the majority of the Ni particles have lost contact to the YSZ after test.

Figure 3A is an LV-SEM micrograph of a pristine Ni–YSZ electrode from a cell of the same type as the cell from which Figures 3B and 3C were taken, but not from the same batch, and therefore the fine-structured active electrode layer can be observed to be thicker in Figure 3A. Figures 3B and 3C are micrographs from a cell tested for 9,000 h at 800 °C with an inlet gas composition of 90% H_2O + 10% H_2. Figure 3B is a piece of the electrode with no current load at the H_2O inlet edge of the cell and with no oxygen electrode on the opposite side, because the oxygen electrode is masked in order to have a 5 mm wide oxygen electrode-free rim zone for sealing purposes. At the steam inlet there is no sealing on top of the Ni–YSZ electrode. Figure 3C shows the same Ni–YSZ electrode, but from a piece of the cell tested at –1 A cm^{-2} (inlet piece of cell with oxygen electrode).

Enrichment in Ni in the form of an increase of big particles is observed in the support near the interface to the active layer in both Figures 3B and 3C, but is most pronounced in Figure 3C. Furthermore, in Figure 3C, which was loaded with –1 A cm^{-2} for 9,000 h at 800 °C, almost all Ni had migrated away from the active layer (notice the increased pore fraction in Figure 3C close to the electrolyte) forming big Ni particles in the support near to the active layer. The pristine electrode (Figure 3A) shows a very well connected population of Ni-particles. Thus, Figure 3 shows that at high water partial pressure without any electrical load only a part of the fine Ni particles in the active layer migrates to the surface of the bigger Ni-particles in the support layer when given enough time (9,000 h). Figure 3C reveals that almost all the fine-structured Ni in the active electrode layer has migrated and been deposited on the bigger grains of the Ni–YSZ support layer.

Figure 4 illustrates that the findings in Figure 3 were not a special case found for two cell tests at one specific set of electrolysis test conditions. The conditions for the tests of the cells from which the electrode samples in Figure 4 were taken were: ~865–875 °C, -2.0 A cm^{-2}, inlet gas: 45% H_2O + 45% CO_2 +10% H_2, and 60% steam + CO_2 conversion. Figure 5 gives the voltage *versus* time curves for the two cells from which the electrode samples were taken.

Figure 4 provides electrode microstructures from two co-electrolysis-tested cells, which were produced by a different procedure than those in Figure 3. The samples also illustrate differences along the fuel flow direction of the cell. A part of the Ni particles have lost their electrical contact to the electrode, which is pointed out by the red arrows in Figures 4B to 4D. By comparison to the pristine electrode (Figure 4A) it is also evident that there is more porosity and less Ni in this region, i.e., Ni must have migrated away. Furthermore, we see that the phenomenon is most pronounced at the steam inlet area of the cell tested for 678 h (Figure 4B), a little less at the outlet of the same cell (Figure 4C), and significantly less at the inlet of the short-term (138 h) test (Figure 4C). In the outlet region of the short-term tested cell, the phenomenon is in its initial phase. The micrographs in Figure 4 are taken from Tao, Ebbesen and Mogensen and Y. Tao's PhD thesis [19, 23]. In fact, the phenomenon has been observed in several other studies at DTU [4–10]. It indicates that the rate of loss of active Ni increases with increasing cell polarization, which is significantly higher in the inlet than in the outlet region due to the high (60%) steam+CO_2 conversion. (Polarization means any kind of potential difference due to losses like electrode overpotential and i*R drop causing Joule heating. Overpotential is always connected to an electrode process). This is because the redox potential of the gas (Nernst voltage) is much more positive at the inlet than at the outlet, which contains much more hydrogen, and the potential of the Ni is close to iso-potential along the whole cell length.

Figure 5 reveals that the degradation looks – as a first rough approximation – to be linear in time, i.e., it does not seem to fade out within the tested period. This behavior of fairly linear degradation during the period from ca. 100–1,000 h of test has been seen in several other tests [8, 10]. The overall cell degradation (Figure 5) only decelerates very little in the time span from ca. 70 h to 700 h for the conditions used

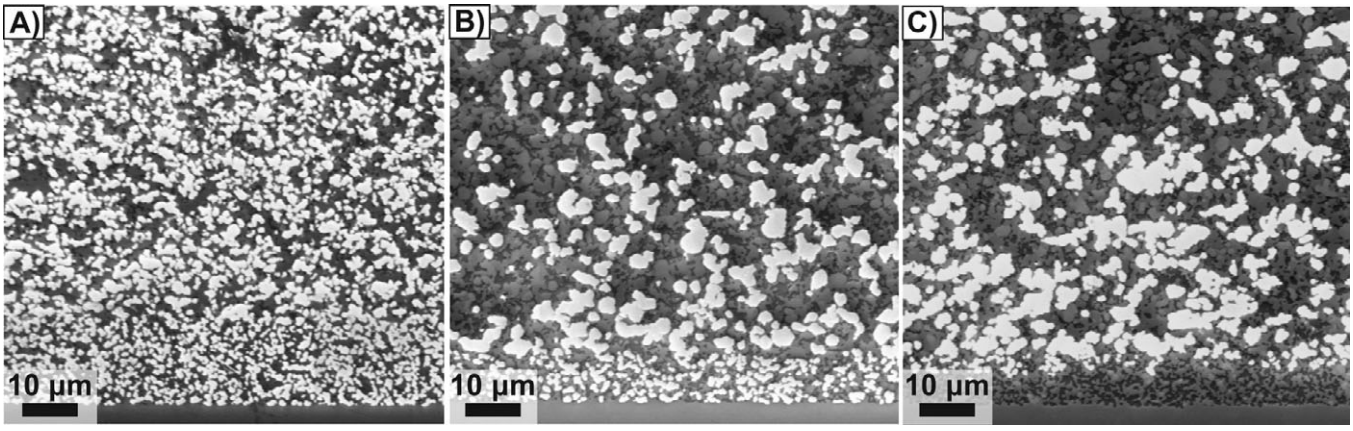

Fig. 3 Representative LV-SEM micrographs from Ni–YSZ electrodes. A) shows a pristine electrode of the same type as the electrodes in B) and C), but not from the same cell batch, and the fine-structured active electrode layer is thicker in A). B) and C) are from a cell tested for 9,000 h at 800 °C applying an inlet gas composition of 90% H_2O + 10% H_2. B) shows a part of the cell with no current load (inlet edge of the cell without oxygen electrode). C) Piece of cell tested at -1 A cm^{-2} (inlet piece of the cell with oxygen electrode).

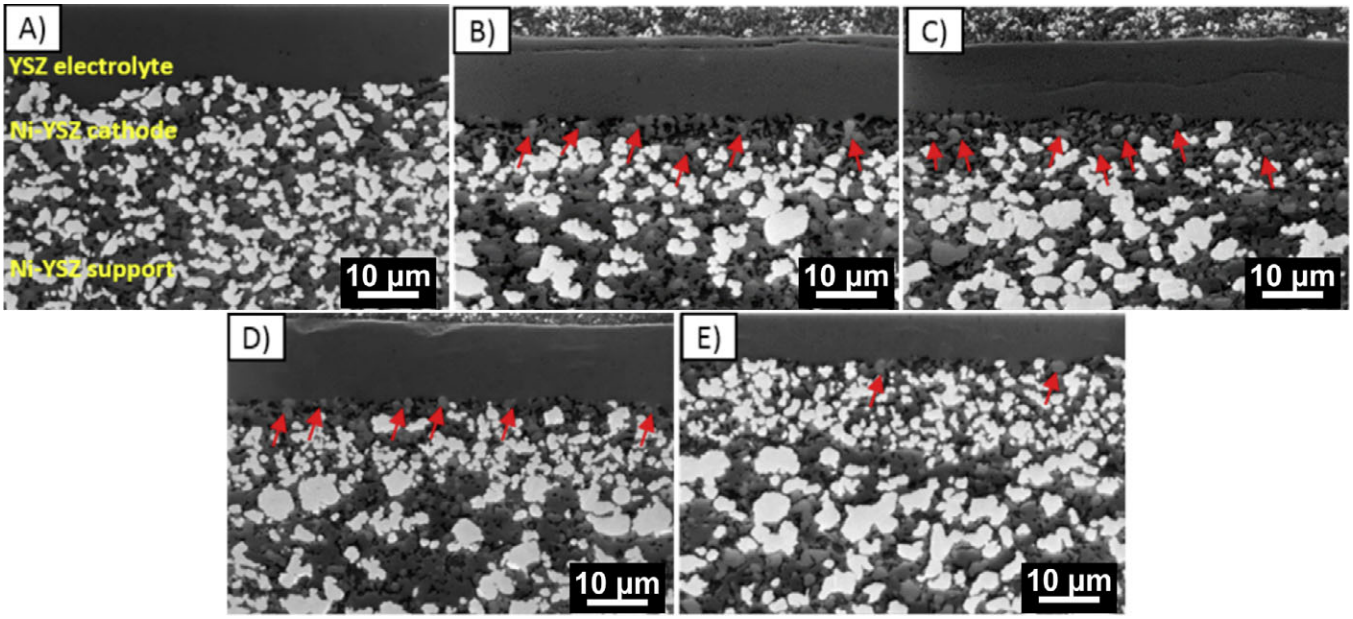

Fig. 4 Low-voltage SEM of Ni–YSZ electrodes in Ni–YSZ cermet supported cells with 8 mol% YSZ electrolyte and LSM-YSZ O_2 electrode. A) a pristine electrode, B) steam + CO_2 inlet and C) outlet area after test with –2.0 A cm^{-2} for 678 h, D) inlet and E) outlet after test of a nominally identical cell with –2.0 A cm^{-2} for 138 h. The initial cell temperature was ~865 °C under operation and finally increased to ~875 °C. Inlet gas: 45 % H_2O + 45 % CO_2 +10 % H_2, 60 % steam + CO_2 conversion. The bright and light gray colors are electrically connected and non-connecting nickel, respectively. The dark gray color is YSZ and black is porosity. The red arrows point out the Ni particles that are not electrically connected. Extra porosity (lost Ni) areas are also visible in this region. For further details see refs. [19, 23]. The Figure is reproduced by permission of Elsevier.

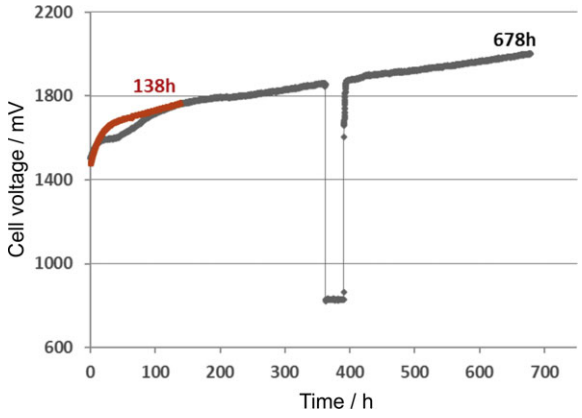

Fig. 5 Cell voltage as a function of time during electrolysis testing. Images of the Ni/YSZ electrodes of the tested cells are presented in Figures. 4B to 4E. Extracted from refs. [19, 23] with permission from Elsevier.

for the electrodes shown in Figure 4 [19, 23]. Of course we are aware that other degradation mechanisms may be in operation in the cell in Figure 5, but as the cathode degradation was the only significant degradation that was identified, we will here assume that the loss of Ni–YSZ particle contact followed by loss of percolation through the network of Ni particles was the only significant degradation mechanism responsible for the degradation seen in Figure 5.

2.2 Fuel Cell Test Results

Figure 6A shows a long known correlation between cell polarization and cell degradation rate [20]. The high polarization at 750 °C and 0.75 A cm^{-2} degrades the cell significantly. Figure 6B shows that a main reason is an extensive loss of contact of Ni in the active electrode to the surrounding Ni, i.e., the electron percolation is partially lost. The loss of electron contact between Ni particles is also often called "loss of electron percolation paths", short "loss of percolation" or non-percolating Ni.

3 Hypotheses

Before going into the description and hypothesis of the migration of Ni we will discuss various reasons for why the contact between Ni and YSZ particles and Ni–Ni particles in the active electrode layer is lost, because the migration of Ni outwards from the electrolyte in SOEC will not start until the contact of Ni and YSZ has been lost.

3.1 The Loss of Contact

Our first question is: why do the Ni particles lose contact to the YSZ particles and to each other?

We hypothesize that the cause of this loss of contact is: (i) partly due to a change in Ni particle shape at very negative potentials due to a change in surface energy with polarization, and (ii) partly due to the effect of humidity, which also pro-

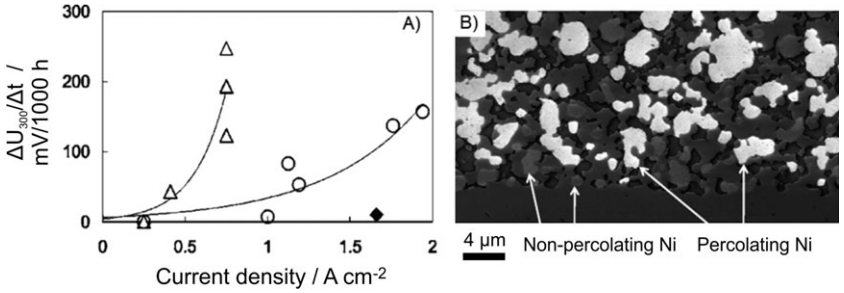

Fig. 6 A) Degradation rate ($\Delta U_{300}/\Delta t$ determined after 300 h) under current load in fuel cell mode as a function of current density and temperature at 750 °C (triangles), 850 °C (circles), and 950 °C (diamonds) [20]. The Figure is reproduced by permission of The Electrochemical Society. B) Low-voltage in-lens SEM image of a similar cell from a durability test for 250 h at 750 °C under similar conditions showing electrically connected (percolating Ni) and electrically isolated Ni (non-percolating) in the active Ni–YSZ electrode layer. The decrease in cell voltage was 70 mV, which is equivalent to 280 mV/1,000 h. [17] The Figure is reproduced by permission of Elsevier.

motes coarsening and rounding of Ni particles by migration of Ni from areas of the particles with a small radius of curvature to areas with a large radius of curvature [24] (and references therein), and partly to contraction of YSZ upon reduction. That the effect of high steam partial pressure itself may cause some loss of contact between Ni particles was also previously reported [24] in accordance with the observed differences between Figures 3A and 3C. Further, it is known that for 8 mol.% YSZ, which is saturated with NiO after sintering of the pre-cermet NiO-YSZ at temperatures of 1,300 °C or above, the YSZ contains about 1 mol.% NiO. When the NiO is reduced out of the YSZ it causes the YSZ lattice to shrink about 0.1 to 0.2 vol.% [25].

Another part of the reason may be that when the Ni–YSZ cermet electrode is polarized very negatively then the YSZ particles will be partially reduced [26]. We assume that in the first stages of this reduction the YSZ will experience a small stoichiometric expansion in analogy with, e.g., ceria reduction [27], but with deeper reduction zirconia will behave different from ceria because in contrast to the rather stable Ce^{3+}, the Zr^{3+} and lower valent Zr ions are not stable. Instead, a kind of solution of oxygen in Zr metal will be formed [28]. This O–Zr "alloy" will expectedly have a smaller molar volume than ZrO_2.

Furthermore, at strongly reducing conditions, interface and grain boundary impurities like SiO_2 will be reduced into Si atoms in Ni, forming a dilute solution. Likewise will ZrO_2 get reduced to metallic Zr in Ni at further negative potentials [4, 29]. The reduction of metal oxide impurities and ZrO_2 into solution in Ni will slightly reduce the molar volume of the oxide part of the cermet (the YSZ skeleton) and leave a little extra porosity around the Ni. This may at least partially cause the loss of contact between Ni particles and between Ni and YSZ particles. Thus, several minor effects may add up and the sum is responsible for the phenomenon of loss of contact between Ni and YSZ particles in the active electrode layer.

Additionally, based on micrographs (Figure 2B) of the Ni–YSZ electrode structures we postulate that the original irregular, elongated Ni particles become more rounded with increasing negative potential, i.e., the surface energy of the Ni increases with progressing more negative potentials at least in the overpotential range down to –400 mV, which may reduce SiO_2 to Si in Ni, but should not reduce ZrO_2. This change in YSZ–Ni interface energy and Ni surface energy from negative (wetting) to positive (de-wetting) due to the strong polarization will cause a loss of Ni–YSZ contact if there is enough space (porosity) for it to happen. It is well-known that electrode polarization will in general change the interfacial energy, but we are aware that it is not *per se* given that it should change the way we suggest here. Yet, we ascribe the loss of percolation to the lower ability of particles to form a connected network if they are all rounded compared to very irregularly shaped particles. If this assumption is correct then the observed spheroidization of Ni particles is supposed to happen through surface diffusion of Ni. This process could be the reason for the initially fast increasing degradation, but also fast decelerating degradation that is seen during the first ca. 70 h in Figure 5 and for most high polarization SOEC tests within the first few hundreds of hours. After this point not much more loss of Ni–YSZ contact takes place in the steam inlet region, but due to the large increase of the local electrolyte resistance (the electric potential loss through the porous YSZ between the new TPB formed further out and the bulk electrolyte surface) the current density will decrease at the inlet and increase further downstream. This redistribution of the current density will continue and is responsible for the further almost linear degradation. In this connection and in particular in the context of Figure 5, it should be noted that the TPB may be inactive in spite of Ni–Ni particle contact if there is no contact between the Ni and the YSZ particles. Figure 7 illustrates proposed mechanisms responsible for the loss of contact between Ni and YSZ particles in the active electrode layer.

A final question to answer in relation to the loss of contact is: why do Ni particles lose contact to each other? We think that this may in part be due to the migration of Ni outwards, as this will start as soon as the Ni contact to the YSZ is lost, because then there is no polarization of the Ni anymore. Actually, if the migration of $Ni(OH)_x$ happens via the gas phase then Ni outside the TPB zone may evaporate, because only Ni inside this zone, i.e. probably within few nanometers of the YSZ, is cathodically polarized. Then, the Ni-particles with the smallest radius of curvature, i.e. the smallest particles and the most irregular parts of bigger particles, will migrate first and at some point, the rest of the Ni-particles will have lost contact to each other. From a technical point of view this seems not very important, as it seems not to happen until after the Ni–YSZ contact has been lost.

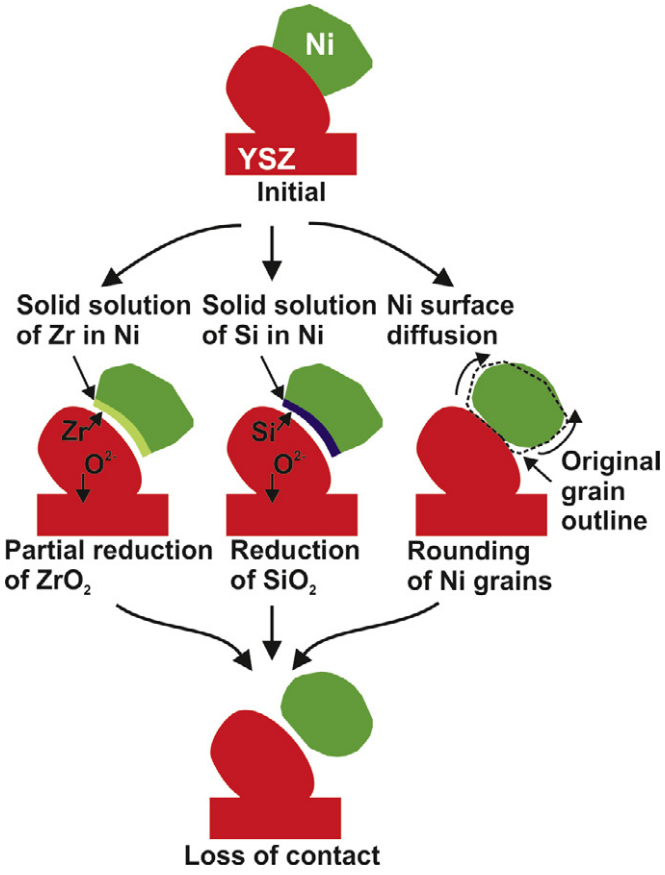

Fig. 7 The envisaged main mechanisms responsible for the loss of contact between Ni and YSZ.

3.2 Migration of Ni away from the Electrolyte

The second question that we must answer is why does Ni migrate away from the YSZ bulk electrolyte opposite to earlier observations in [1]? To answer this, we have to look at the driving forces in the system after Ni has lost contact to the YSZ.

Intuitively, we would think that Ni would always migrate down the steam partial pressure (pH_2O) gradient as previously observed [1], but in the present cases, Ni seems to migrate up the pH_2O gradient. However, it is also observed that there is a preceding phase in this Ni–YSZ electrode degradation, namely that the Ni particles closest to the YSZ electrolyte lose contact to each other as described above. This means that the active three phase boundary (TPB) moves away from the electrolyte and causes a significant increase in the ohmic resistance as is also observed in electrochemical impedance spectra, i.e. the main degradation of $R_{p,Ni}$ takes place during the ca. 300 h period where the loss of contact happens. In one case, where a cell was operated at –1 A cm^{-2}, we see that the electrode polarization, $R_{p,Ni}$, increases to ca. 400 mΩ cm^2 implying an overpotential of ca. –400 mV (electrode overpotential for both electrodes, but the major part is from the Ni–YSZ) before the series resistance, R_s, starts to increase. (R_s originates from the electrolyte resistance). Here, it should be borne in mind that even though the Ni–YSZ has lost contact, the R_s value as measured by impedance spectroscopy may not change, because as long as the gap between the Ni and the YSZ is small enough then the capacitance associated with this gap may be effectively zero at high frequency. In contrast R_p will increase drastically as soon as the Ni–YSZ contact is lost because it will not be possible to transfer an oxide ion across even a 1 Å gap, i.e., the local polarization resistance at a given Ni–YSZ contact point goes towards infinity as soon as the intimate atomic contact is lost [10]. It should also be noted that the mentioned 300 h is not a number with any general meaning for Ni–YSZ electrodes. It totally depends on the active electrode structure [10].

Before the loss of contact of the Ni and YSZ particles, the Ni will migrate towards the YSZ electrolyte during negative polarization. Depending on the exact operating conditions, the Ni particles may lose contact before much migration has taken place. If this happens, there will be no pH_2O gradient in the volume between the active TPB (now moved away from the electrolyte) and the electrolyte as illustrated in Figure 6. Furthermore, the potential of the non-contacted Ni particles will be determined simply by the steam/hydrogen ratio, while the Ni at the TPB is significantly negatively polarized, i.e., there is a clear electrochemical potential difference between them. The migration of Ni has been reported to take place in form of Ni–OH complexes in the family of $Ni(OH)_x$, but maybe with Ni in a lower oxidation state than +2 [15, 16] even though migration of volatile $Ni(OH)_2$ has be reported for fuel cell mode operation [17]. Anyway, the activity of Ni in a positive oxidation state will be lowest at the most reducing condition, i.e., at the most active TPB some distance (max. a few microns) away from the electrolyte. Consequently, the Ni diffuses, probably in the gas phase, to the active TPB where it precipitates. This will cause the Ni particles at the TPB (which is now a little away from the electrolyte) to grow, and this is actually observed. At some stage a significant increase in Ni particle size at the active TPB has taken place and no loss of contact between them will then happen, but thereafter a too dense Ni layer may form.

Figure 8 shows the three important parameters for the Ni migration as a function of distance from the bulk electrolyte into the SOEC cathode. They are the Ni overpotential, η, the activity of Ni–OH species, $a_{Ni(OH)x}$, and the steam partial pressure, pH_2O.

This explains that the rate of outwards migration of Ni is higher at the inlet than at the outlet. The migration rate increases with increasing overpotential, which is significantly higher at the inlet than in the outlet region due to the high (60%) steam+CO_2 conversion. This is due to the fact that the electrical potential of the Ni is close to iso-potential along the whole cell length, but the redox potential of the gas (Nernst potential) is much more positive at the inlet than at the outlet, which contains much more hydrogen than the inlet gas does.

Figure 9 sketches the three most important situations that we have observed in Figures 2 and 3, which are the basis for our hypothesis and which explains the observations presented in Figure 4.

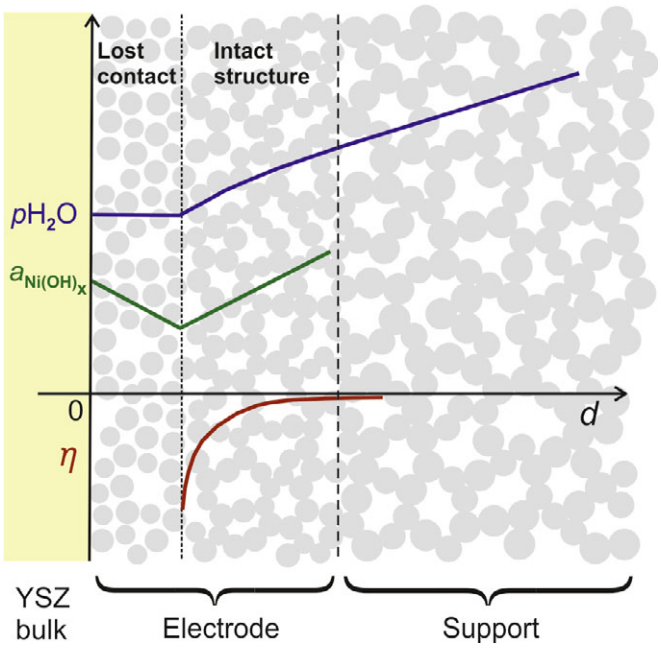

Fig. 8 A sketch of the qualitative variation of the three important parameters from the surface of the bulk electrolyte ($d = 0$) through the two zones of the as-fabricated SOEC active cathode (A-layer), which has separated into a zone with partially lost contact between Ni and YSZ particles and an intact structure zone. It represents the stage of degradation seen in Figure 2B. d is the distance from the bulk YSZ electrolyte, η is the local overpotential of Ni particles, $a_{Ni(OH)x}$ is the activity of Ni–OH species, and pH_2O is steam partial pressure.

In the case of SOFC mode the $Ni(OH)_x$ is expected to migrate away from the electrolyte and the active TPB zone as both the potential gradient and the steam gradient have direction away from the electrolyte. However, the data in Figure 6A indicates that the potential gradient is much more important for the Ni migration than the steam gradient is. The overpotential, and *via* this the electrochemical potential gradient, is very temperature dependent (high activation energy of ca. 0.8 eV) at a given current density, whereas the diffusion of steam has a rather small dependency on temperature. Further, the silica glassy impurities, which may be found at the Ni–YSZ interface, will also migrate away with the steam gradient [30] and even though this is advantageous in freeing TPBs it may, on other hand, also contribute to losing the contact between Ni and YSZ.

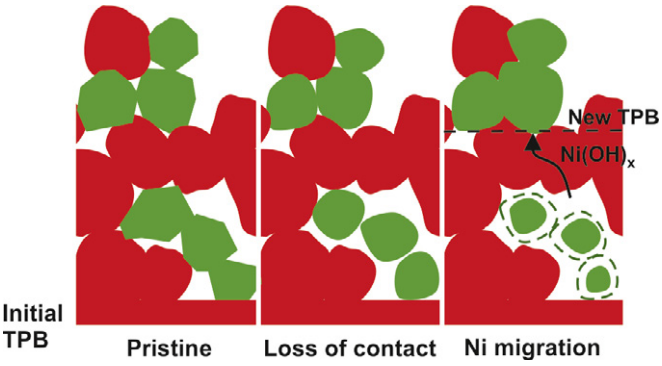

Fig. 9 Illustration of the mechanisms with the three main phases of the Ni migration outwards from the electrolyte in SOEC mode.

It is known that the surface energy varies more or less symmetrical around the "zero charge" potential also called the zero zeta potential [31]. Thus, the effect of overpotential on losing the Ni–YSZ contact might be similar in the SOFC and SOEC modes. If this is the correct explanation it means that the zero charge potential should lie not too far from the open circuit electrode potential of our H_2/Ni–YSZ electrodes.

The much higher influence of temperature on the overpotential and potential gradients than on the steam gradient seems able to explain the difference between the results in [1], the migration of Ni towards the TPB at 950 °C in contrast to the results seen in Figures 3 and 4 at 800 and 870 °C, respectively. At 950 °C the overpotential becomes quite small and therefore the Ni–YSZ interface energy change is much smaller, and the Ni–YSZ contact remains good. The steam driven $Ni(OH)_x$ migration towards the electrolyte and the reduction kinetics at the intact TPBs in the electrolysis mode will be faster at the high temperature resulting in a blockade of the porosities of the active electrode layer with Ni, as observed in [1].

4 Conclusions

We described a new set of degradation mechanisms of highly negatively polarized Ni–YSZ cermet electrodes and offered explanations for the processes that cause the degradation. Our hypothesis predicts that the only safe way of avoiding this degradation is to avoid that the Ni–YSZ cermet electrode is polarized too much. However, we are not able to give a maximum cell voltage for this because we do not yet have a quantitative description of the loss of contact between the Ni–YSZ and between the Ni particles. This will require the construction of a full thermodynamic mathematical model, which will be future work. Furthermore, the cell voltage will depend much on the polarization resistance of the electrolyte and the anode apart from the polarization resistance of the cathode itself, i.e., will depend on cell design, precise composition of cell materials, electrode microstructure etc.

Acknowledgements

This work was financially supported by Energinet.dk through the project ForskEL 2015-1-12276 "Towards Solid Oxide Electrolysis Plants in 2020", by the Energy Technology Development and Demonstration Programme (EUDP) under the Danish Energy Agency *via* the project "Green Natural Gas", and by the DTU Mobility Fellowship Program. We are grateful to Dr. Torben Jacobsen for valuable discussion.

References

[1] A. Hauch, S. D. Ebbesen, S. H. Jensen, M. Mogensen, *J. Electrochem. Soc.* **2008**, *155*, B1184.

[2] S. D. Ebbesen, S. H. Jensen, A. Hauch, M. B. Mogensen, *Chem. Rev.* **2014**, *114*, 10697.

[3] R. Knibbe, M. L. Traulsen, A. Hauch, S. D. Ebbesen, M. Mogensen, *J. Electrochem. Soc.* **2010**, *157*, B1209.

[4] M. Chen, Y. L. Liu, J. J. Bentzen, W. Zhang, X. Sun, A. Hauch, Y. Tao, J. R. Bowen, P. V. Hendriksen, *J. Electrochem. Soc.* **2013**, *160*, F883.

[5] X. Sun, M. Chen, P. V. Hendriksen, M. B. Mogensen, *Proc. 11th European SOFC & SOE Forum*, (Eds. N. Christiansen, J. B. Hansen), European Fuel Cell Forum AG, Lucerne, Switzerland, **2014**, Chapter 16, pp. 41–51.

[6] P. Hjalmarsson, X. Sun, Y.-L. Liu, M. Chen, *J. Power Sources* **2014**, *262*, 316.

[7] X. Sun, A. D. Bonaccorso, C. Graves, S. D. Ebbesen, S. H. Jensen, A. Hagen, P. Holtappels, P. V. Hendriksen, M. B. Mogensen, *Fuel Cells* **2015**, *15*, 697.

[8] A. Hauch, F. Karas, K. Brodersen, M. Chen, *Proc. 11th European SOFC & SOE Forum*, (Eds. N. Christiansen, J. B. Hansen), European Fuel Cell Forum AG, **2014**, Chapter 12, pp. 88–97.

[9] S. D. Ebbesen, X. Sun, M. B. Mogensen, *Faraday Discuss.* **2015**, *182*, 393.

[10] A. Hauch, K. Brodersen, M. Chen, M. B. Mogensen, *Solid State Ionics* **2016**, *293*, 27.

[11] F. Tietz, D. Sebold, A. Brisse, J. Schefold, *J. Power Sources* **2013**, *223*, 129.

[12] J. Schefold, A. Brisse, H. Poepke, *Electrochim. Acta* **2015**, *179*, 161.

[13] M. S. Sohal, J. E. O'Brien, C. M. Stoots, V. I. Sharma, B. Yildiz, A. Virkar, *J. Fuel Cell Sci. Tech.* **2012**, *9*, 011017–1.

[14] J. Sara, J. Schefold, A. Brisse, E. Djurado, *Electrochim. Acta* **2016**, *201*, 57.

[15] J. Sehested, J. A. P. Gelten, I. N. Remediakis, H. Bengaard, J. K. Nørskov, *J. Catal.* **2004**, *223*, 432.

[16] J. Sehested, J. A. P. Gelten, S. Helveg, *Appl. Catal. A* **2006**, *309*, 237.

[17] A. Hauch, P. S. Jørgensen, K. Brodersen, M. Mogensen, *J. Power Sources* **2011**, *196*, 8931.

[18] A. Gubner, H. Landes, J. Metzger, H. Seeg, R. Strüber, *Proc. Solid Oxide Fuel Cells V*, (Eds. M. Dokiya, O. Yamamoto, H. Tagawa, S. C. Singhal), The Electrochemical Society Proceedings Series, Pennington, NJ, USA, **1997**, *PV 97-40*, pp. 844–850.

[19] Y. Tao, S. D. Ebbesen, M. B. Mogensen, *J. Power Sources* **2016**, *328*, 452.

[20] A. Hagen, R. Barfod, P. V. Hendriksen, Y.-L. Liu, S. Ramousse, *J. Electrochem. Soc.* **2006**, *153*, A1165–A1171.

[21] K. Thydén, Y. L. Liu, J. B. Bilde-Sørensen, *Solid State Ionics* **2008**, *178*, 1984.

[22] K. Brodersen, A. Hauch, M. Chen, J. Hjelm, *European Patent Application No 1518138.3*, **2015**.

[23] Y. Tao, *PhD thesis*, DTU Energy, Technical University of Denmark **2013**, p. 115.

[24] M. H. Pihlatie, A. Kaiser, M. Mogensen, M. Chen, *Solid State Ionics* **2011**, *189*, 82.

[25] S. Linderoth, N. Bonanos, K. V. Jensen, J. B. Bilde-Sørensen, *J. Am. Ceram. Soc.* **2001**, *84*, 2652.

[26] J. H. Park, R. N. Blumenthal, *J. Electrochem. Soc.* **1989**, *136*, 2867.

[27] S. R. Bishop, D. Marrocchelli, C. Chatzichristodoulou, N. H. Perry, M. B. Mogensen, H. L. Tuller, E. D. Wachsman, *Annu. Rev. Mater. Res.* **2014**, *44*, 205.

[28] M. Chen, B. Hallstedt, L. J. Gauckler, *Solid State Ionics* **2004**, *170*, 255.

[29] C. Chatzichristodoulou, M. Chen, P. V. Hendriksen, T. Jacobsen, M. B. Mogensen, *Electrochim. Acta* **2016**, *189*, 265.

[30] A. Hauch, S. H. Jensen, J. B. Bilde-Sørensen, M. Mogensen, *J. Electrochem. Soc.* **2007**, *154*, A619.

[31] K. J. Vetter, *Electrochemical Kinetics*, Academic Press, London, **1967**, pp. 73–87.